Energy Transfer from Luminescent Porous Silicon to Adsorbed Osmium(II) and Ruthenium(II) Polypyridyl Complexes

Durwin R. Striplin,[†] Craig G. Wall,[‡] Bruce W. Erickson, and Thomas J. Meyer*

Department of Chemistry, University of North Carolina at Chapel Hill, Chapel Hill, North Carolina 27514

Received: September 17, 1997; In Final Form: December 17, 1997

Surface adsorption of transition-metal polypyridyl complexes on highly luminescent, anodized porous silicon (p-Si) wafers leads to dramatic quenching of the emission. Facile energy transfer occurs from the surface to adsorbed complexes of Ru^{II} and Os^{II}. Photoluminescence (PL) from underivatized p-Si is excitation- and monitoring-wavelength-dependent. A phenomenological model is proposed to explain these observations in which intercluster energy transfer occurs by an energy-transfer cascade, and there is weak kinetic coupling to even lower-energy surface emitters. Adsorption of $[Zn(dmb)_3](PF_6)_2$ (dmb is 4,4′-dimethyl-2,2′-bipyridine) or *fac*-$[Re(bpy)(CO)_3(4\text{-Etpy})](PF_6)_2$ (bpy is 2,2′-bipyridine; 4-Etpy is 4-ethylpyridine), possibly by ion-exchange, results in quenching of the low-energy surface emitters. For adsorbed $[M^{II}(bpy)_2(4\text{-}CO_2H\text{-}4'Mebpy)](PF_6)_2$ (M = Ru, Os; 4-CO_2H-4′Mebpy is 4-carboxylic acid-4′-methyl-2,2′-bipyridine), p-Si* → M^{II} energy transfer occurs to low-lying metal-to-ligand charge-transfer (MLCT) excited states on the complexes as revealed by excitation and emission measurements. Energy transfer is efficient (>90%) and more rapid for Os^{II} ($k_{en} \approx 6 \times 10^6\ s^{-1}$) than for Ru^{II} by a factor of ∼10, consistent with a decrease in driving force for p-Si* → M^{II} energy transfer.

Introduction

Following the report by Canham et al.[1] of visible photoluminescence (PL) from microporous silicon (p-Si), much effort has been directed toward understanding the PL mechanism. Some of the suggestions that have been made are nanocrystalline quantum confinement and recombination of excitons, surface-siloxene formation, surface hydride passivation, surface-state mechanisms, and amorphous Si:H lattice rearrangement.[2−10] The most common methods of fabricating these p-Si films are anodic etching in solutions containing HF and nonbiased chemical etching in HF/HNO_3 solutions. The resulting PL characteristics depend on the etching conditions. Typically, a broad featureless emission is observed at room temperature centered at 550−800 nm with full width at half-maximum of ∼200 nm.[11]

Sailor et al.[12] compared reversible quenching of the PL from p-Si exposed to organic solvents with p-Si samples that were hydrogen-passivated and hydrophobic and concluded that the PL is extremely surface-sensitive. All of the solvents examined reduced the emission intensity of p-Si, suggesting that solvent interactions increase nonradiative decay. A correlation was observed between the extent of quenching and the solvent dipole moment. The molecules, a series of polycyclic aromatic molecules, were also chosen to discriminate among electron-, hole-, and energy-transfer mechanisms and allowed them to conclude that these molecules probably quench p-Si photoluminescence predominantly via an energy-transfer mechanism.[13] Bocarsly and co-workers[14] found that reversible quenching of the PL occurred by exposing p-Si to inorganic and organic bases. They concluded that emission from p-Si is associated with the presence of a relatively acidic ground-state surface proton. Canham[15] has shown that p-Si can be used as a scaffold for laser dyes. This approach, however, does not use the intrinsic PL of the p-Si but simply involves oxidation of the p-Si layer to SiO_2 and coating the p-Si layer with a laser dye by solution evaporation. This technique yields a highly porous glass impregnated with the laser dye. Meyer and Ko[16] have demonstrated that solutions containing electron or energy-transfer quenchers diminish the luminescence of hydrogen-terminated p-Si. Sweryda-Krawiec and Coffer[17] studied the impact of photooxidation of p-Si on the ability of EPh_3 (E = N, P, As) in heptane solutions to quench the PL. For a given substrate the degree of quenching followed the gas-phase proton affinities of the triaryl quencher. Upon surface oxidation, a measurable decrease in the quenching of the PL was observed in the presence of the triaryl derivatives. Other reports have described the quenching of p-Si PL by metal ions such as Cu^{2+}, Ag^+, and Au^{3+}, all of which are reducible at accessible potentials.[18,19] Quenching of the p-Si emission occurred upon immersion in dilute solutions of the metal ions and by the adsorbed ions left on the surface after evaporation. A review of molecular quenching of luminescent p-Si complexes has been published by Coffer.[20]

The electron transfer and excited-state properties of the complexes $[M(bpy)_2(4\text{-}CO_2H\text{-}4'Mebpy)]^{2+}$ (M = Ru, Os; bpy is 2,2′-bipyridine; 4-CO_2H-4′Mebpy is 4-carboxylic acid-4′-methyl-2,2′-bipyridine) have been investigated on ITO (In_2O_3:Sn) and SnO_2:Sb electrodes and on glass and powdered silica surfaces.[21,22] The complexes can be oxidized and reduced and have low-lying metal-to-ligand charge transfer (MLCT) excited states,

$$M^{II}(bpy)_3^{2+} \xrightarrow{h\nu} M^{III}(bpy^{\bullet -})(bpy)_2^{2+*} \qquad (1)$$

which undergo both facile electron and energy transfer. For the carboxylic acid derivatives, spectroscopic evidence has been found for ester (**1**) or H-bond (**2**) formation to the oxide surfaces. These links are hydrolytically unstable.

[†] Department of Chemistry, Davidson College, Davidson, NC.
[‡] Department of Chemistry, University of Illinois at Urbana−Champaign, Urbana, IL.

S1089-5647(97)03057-5 CCC: $15.00
Published on Web 03/06/1998

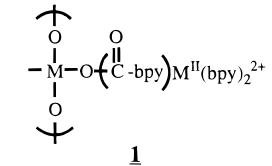

1

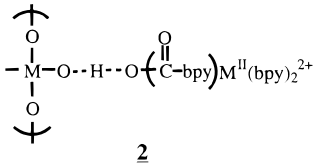

2

On semiconductor electrodes these MLCT excited states are rapidly and efficiently quenched. On TiO_2, quenching occurs by rapid photoinjection into the conduction band. When combined with band-bending, this has provided a basis for a family of photovoltaic solution devices.[21] On glass surfaces containing both complexes and quenchers, rapid cross-surface electron and energy transfer have been shown to occur.[22]

Excited-state energies for the polypyridyl complexes can be varied widely depending on the metal and the chromophoric and nonchromophoric ligands. In the sequence $[Re(bpy)(CO)_3(4\text{-Etpy})]^{+*}$ (4-Etpy is 4-ethylpyridine), $[Ru(bpy)_2(4\text{-}CO_2H\text{-}4'Mebpy)]^{2+*}$, and $[Os(bpy)_3]^{2+*}$, in acetonitrile at room temperature, emission energies are 2.1, 1.9, and 1.6 eV. This series spans the range of luminescence energies from porous silicon with the Re^{I} complex on the high-energy side and the Os^{II} complex on the low-energy side. When surface-adsorbed, the possibility exists for a dynamic interplay between the excited and ground states of these molecules, and surface or quantum-confined emitters in the porous silicon.

The goals of this study were twofold. One was to provide possible insight into the origin of the emission from p-Si. The second was to explore the photophysical properties of hybrid materials prepared by surface adsorption of polypyridyl complexes. Oxidatively etched p-Si was chosen as the substrate, since surface hydroxyl groups could provide a basis for surface adsorption of carboxylic acid derivatives by ester formation (**1**) or H-bonding (**2**). The structures of the ligands and organic molecules used in this study are illustrated below.

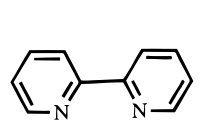

bpy

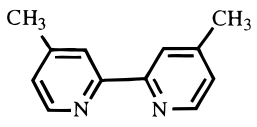

dmb

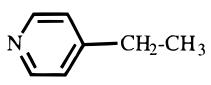

4-Etpy

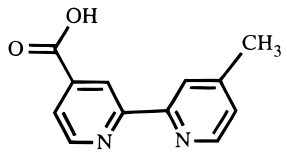

4-CO_2H-4'Mebpy

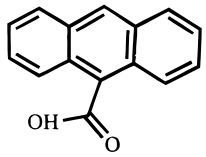

9-AncO_2H

Experimental Section

Fabrication of Porous Silicon Surfaces. The silicon substrate for p-Si fabrication was purchased from Virginia Semiconductor or EL-CAT Semiconductor as Czochralski-grown wafers in ⟨100⟩ orientation, n-type (P-doped) with 0.1−10 Ω cm resistivity. The wafers were anodized in 1:1 (v/v) ethanol−48% HF in water. The Si was etched by using a current density of 20 mA/cm^2 for 20 min. The electrochemical cell was a Teflon single-compartment cell designed for lateral anodization as described by Jung et al.[23] The potentiostat was an EG&G Princeton Applied Research model 173 with a model 175 waveform generator. Samples were transferred to Teflon wafer storage containers (Fluoroware) and stored under ambient conditions for 1 week and sealed with Parafilm until spectroscopic measurements were conducted.

Surface Derivatization. The surfaces of anodized p-Si wafers were rinsed with HPLC-grade water (Fisher) and UV-grade acetonitrile (Burdick and Jackson) and dried under a stream of argon. The freshly dried wafers were soaked in solutions ($0.5-1) \times 10^{-3}$ M in PF_6^- salts of the complexes for 24 h, rinsed with acetonitrile, dried under a stream of argon, and stored in containers. This procedure was used to prepare derivatized surfaces containing adsorbed $[M(bpy)_2(4\text{-}CO_2H\text{-}4'Mebpy)](PF_6)_2$ (M = Ru,Os),[24] 4-CO_2H-4′Mebpy,[24] 9-AncO_2H (Aldrich), $[Os(bpy)_3](PF_6)_2$,[25] *fac*-$[Re(bpy)(CO)_3(4\text{-Etpy})](PF_6)$,[26] and $[Zn(dmb)_3](PF_6)_2$ (dmb is 4,4′-dimethyl-2,2′-bipyridine).[27]

Spectroscopy. Each sample was characterized by steady-state excitation and emission measurements and by time-resolved photoluminescence spectroscopy before and after derivatization. Emission and excitation spectra were obtained with a SPEX Fluorolog F212 spectrofluorometer operated in the photon-counting mode with a cooled Hamamatsu R666 photomultiplier tube corrected for detector sensitivity. Time-resolved emission decays were observed following pulsed excitation from a PRA LN102 tunable dye laser pumped by a PRA LN100 nitrogen laser. The emitted light was observed at an angle of 45° with respect to the defocused excitation light beam (22° to the sample surface), passed through appropriate Oriel band-pass filters to eliminate excitation scatter, and dispersed with a Macpherson 272 scanning monochromator. The emission was monitored with a Hamamatsu R446 PMT photomultiplier−LeCroy 7200 transient digitizing oscilloscope combination interfaced to a PC. Time-resolved emission spectra were obtained with the same laser excitation source, but the emitted light was dispersed through a Jarrell-Ash MonoSpec 27 monochromator (150 groves/mm, 450 nm blazed grating) and the spectral pattern monitored by a Princeton Instruments IRY-700G optical multichannel analyzer, OMA, operating in the gated mode with a ST-110 OSMA detector-controller. Synchronization of the excitation pulse and OMA exposures was controlled by a BNC model 7010 digital delay generator and a Princeton Instruments FG-100 pulse generator.

Results

Underivatized Porous Silicon. Emission and excitation spectra from a typical oxidatively etched p-Si surface are shown in Figure 1. Emission band shapes and energies are sample-dependent. In the samples produced for this study, emission maxima ranged from 650 to 710 nm. The data in the figure are for a single, representative p-Si sample. At room temperature, the emission is excitation-dependent with the maximum shifting to the red upon lower-energy excitation. The exponential tail into the visible in the excitation spectra is typical of the Urbach absorption edges of amorphous or disordered

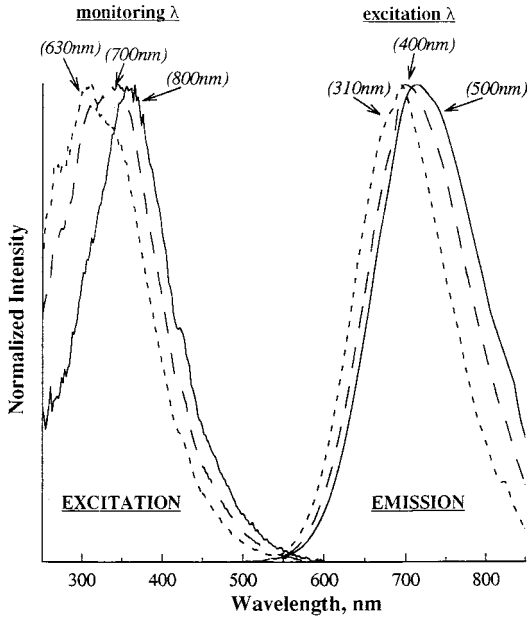

Figure 1. Normalized room-temperature emission and excitation spectra for oxidatively etched p-Si. The excitation spectra were acquired at monitoring wavelengths 630 nm (- - -), 700 nm (— — —), and 800 nm (—). Emission spectra were acquired following excitation at 310 nm (- - -), 400 nm (— — —), and 500 nm (—).

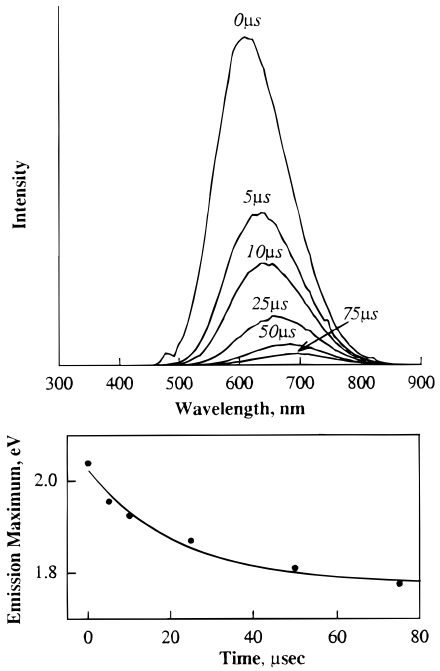

Figure 2. Time-resolved PL spectra of p-Si as in Figure 1 measured at 0, 5, 10, 25, 50, and 75 μs after excitation at room temperature following laser excitation at 337 nm. The bottom figure replots the data (●) as energy maxima vs time. A fit (—) of the data to eq 2 with $E_r = 0.25$ eV, $M_f = 1.78$ eV, and $\tau_L = 22$ μs is also shown.

semiconductors.[28] Our observations are consistent with the results of earlier studies on luminescent p-Si.[5,29,30]

Emission decay lifetimes were in the range 10−100 μs and nonexponential at all monitoring wavelengths. Average lifetimes increased as the monitoring energy wavelength was increased. As illustrated in Figure 2, the emission maximum is time-dependent with the emission maximum shifting to lower energy (higher wavelength) with time, consistent with previous observations.[29−32] The relaxation time for the emission maximum, τ_L, was obtained by fitting the data to eq 2:

$$M(t) = E_r \exp(-t/\tau_L) + M_f \quad (2)$$

In eq 2, $M(t)$ is the emission maximum at time t, E_r is the relaxation energy (the difference in emission energy between $t = 0$ and $t = \infty$), and M_f the final emission maximum. The fit of the data to this expression with $E_r = 0.25$ eV, $M_f = 1.78$ eV, and $\tau_L = 22$ μs ($k_L \approx 4 \times 10^4$ s^{-1}) is shown in Figure 2.

Kinetic decays from p-Si have been fit by others[16,29,33−35] with the Kohlrausch−Williams−Watts distribution function in eq 3.[36−39] It expresses the intensity change with time, $I(t)$, as a probability-limiting distribution of lifetimes rather than as a sum of exponential decays:

$$I(t) = I_0 \exp[-(t/\tau)^{\beta}] \quad (3)$$

The parameters τ and β are the lifetime and nonexponentiality factor, respectively, and I_0 the emission intensity at $t = 0$. For $\beta = 1$ the distribution is a delta function and decay is exponential with a single value for τ. For $\beta < 1$ there is a distribution of lifetimes with β proportional to the width of the distribution.[40,41]

Results obtained by application of eq 3 to PL from p-Si are shown in Figure 3 where τ and β are plotted as a function of monitoring wavelength for excitation at 372 or 471 nm. With excitation at 372 nm, β is nearly constant ($\beta = 0.7$) across the emission and τ decreases with increasing emission energy. With visible excitation at 471 nm, τ and β vary in a complex way across the emission: τ and β rise to a maximum at ∼1.8 eV and then decrease at lower energy. The absolute magnitudes of τ and β are sample-dependent, but the trends in monitoring and excitation dependence are general.

Adsorbed Os^{II}. The p-Si sample described in the previous section was derivatized with $[Os(bpy)_2(4\text{-}CO_2H\text{-}4'Mebpy)](PF_6)_2$ giving p-Si−Os^{II}. Emission and excitation spectra of the resulting modified surface are shown plotted as a function of excitation wavelength in Figure 4. Emission from p-Si was quenched by >95%, and a new emission observed with the band maximum shifted almost 100 nm to the red of the original p-Si emission. There is an increase in p-Si emission on the high-energy side with high-energy excitation at 310 nm. The excitation spectrum monitored at the blue edge of the emission (at 650 nm) included an Urbach edge. Monitoring at 800 nm provided clear evidence for adsorbed Os^{II} by the appearance of a shoulder at ∼480 nm, which nearly coincides with an MLCT absorption maximum of the Os^{II} complex in CH_3CN at 470 nm.

Emission decays were on the order of nanoseconds, almost 6 orders of magnitude shorter than emission from underivatized p-Si. Better fits of the emission lifetimes were obtained by using the biexponential decay function in eq 4 rather than eq 3:

$$I(t) = I_0 \exp(-t/\tau_1) + (1 - I_0) \exp(-t/\tau_2) \quad (4)$$

In this equation τ_1 (=k_1^{-1}) and τ_2 (=k_2^{-1}) are kinetic constants. Application of eq 4 to PL decay from the modified surface gave $\tau_1 \approx 23$ ns ($k_1 \approx 4.3 \times 10^7$ s^{-1}) and $\tau_2 \approx 165$ ns ($k_2 \approx 6.1 \times 10^6$ s^{-1}). These values are somewhat excitation- and monitoring-wavelength dependent. In Figure 5 are shown plots of the fraction of emission by the longer-lived component as a function of excitation and emission wavelengths. These data show that the longer-lived component is favored at higher emission energies and with higher energy excitation. For 350-nm excitation the percentage of the long-lived component follows the underivatized p-Si emission profile reasonably well.

After photophysical characterization, the derivatized sample was washed with acetonitrile, water, and methanol, soaked in

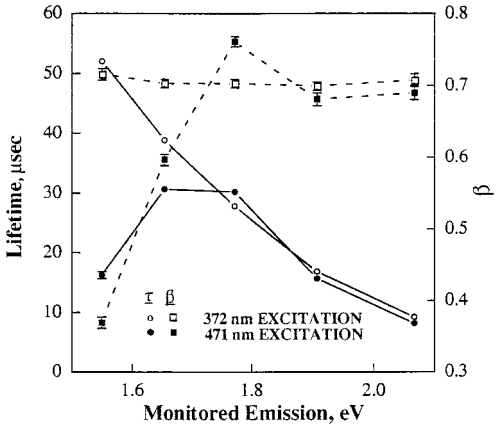

Figure 3. Lifetime τ (○ or ●) and exponential factor β (□ or ■) from fits of PL decay from p-Si according to eq 3. Variations in τ and β as a function of monitoring energy are shown for excitation at 372 nm (○, □) and 471 nm (●, ■).

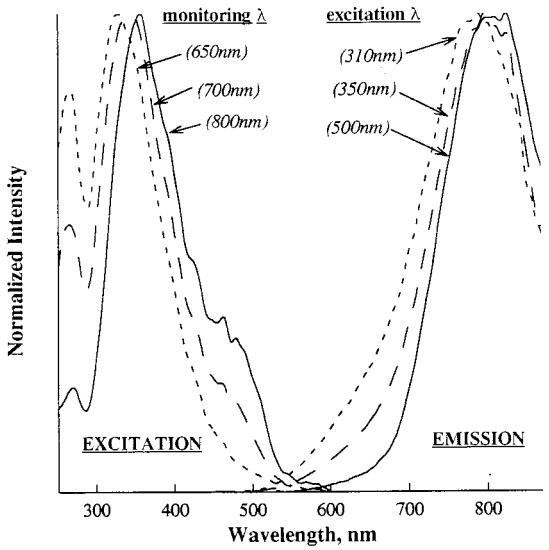

Figure 4. Normalized room-temperature emission and excitation spectra of p-Si derivatized with $[Os(bpy)_2(4\text{-}CO_2H\text{-}4'Mebpy)](PF_6)_2$. Emission was monitored at 650 nm (- - -), 700 nm (— — —), and 800 nm (—) for the excitation spectra. Excitation wavelengths for the emission spectra were 310 nm (- - -), 350 nm (— — —), and 500 nm (—).

methanol for 24 h, and sonicated in methanol for 5 min to remove as much of the Os^{II} complex as possible without damaging the surface. Almost 90% of the original emission intensity was recovered after stripping.

A p-Si wafer was derivatized with $[Os(bpy)_3](PF_6)_2$, which has no carboxylic acid functional group. The emission, excitation, and decay properties of this surface were qualitatively similar to those of the $[Os(bpy)_2(4\text{-}CO_2H\text{-}4'Mebpy)](PF_6)_2$ derivatized sample. The extent of quenching was less (~90%), and emission was red-shifted by only 60 nm. In biexponential fits of the decay data the average lifetime of the long-lived component was an order of magnitude greater and constituted a greater percentage of the light emitted from the sample.

Ru(II) Derivatized Sample. Emission and excitation spectra of p-Si and p-Si derivatized with $[Ru(bpy)_2(4\text{-}CO_2H\text{-}4'Mebpy)](PF_6)_2$ (p-Si−Ru^{II}) are shown in Figure 6. Emission was ~80% quenched upon derivatization. With excitation at 310 nm, PL from p-Si−Ru^{II} was slightly red-shifted compared with that from p-Si and there was a slight increase in bandwidth. Excitation at 370 nm resulted in a slight blue shift in PL from

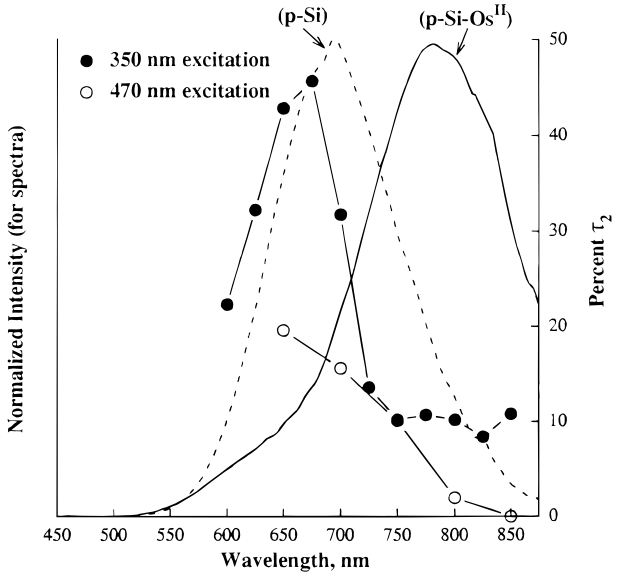

Figure 5. Percentage of emission by the τ_2 p-Si (165-ns) component by applying eq 4 to PL decay from p-Si derivatized with $[Os(bpy)_2(4\text{-}CO_2H\text{-}4'Mebpy)](PF_6)_2$. The data are shown as a function of monitoring wavelength with excitation at 350 nm (●) or 470 nm (○). Normalized emissions from underivatized p-Si (- - -) and derivatized p-Si (—) with 310-nm excitation are shown for reference.

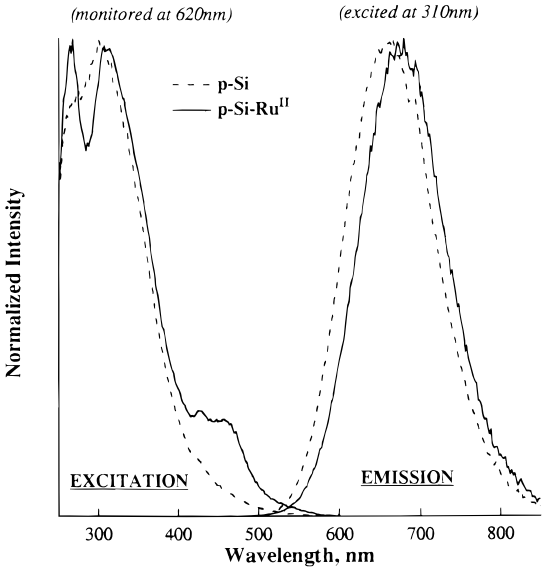

Figure 6. Normalized room-temperature emission and excitation spectra of p-Si (—) and p-Si derivatized with $[Ru(bpy)_2(4\text{-}CO_2H\text{-}4'Mebpy)](PF_6)_2$ (- - -). The excitation spectrum was acquired by monitoring emission at 620 nm and the emission spectrum by excitation at 310 nm.

p-Si−Ru^{II} (Figure 7a). With excitation at 450 nm the two emissions almost coincide with p-Si−Ru^{II} slightly to the blue (Figure 7b). As for p-Si−Os^{II}, an MLCT absorption feature for the complex appears in the excitation spectrum as a shoulder at ~480 nm. This feature coincides with λ_{max} = 478 nm for the complex in CH_3CN and is not present in p-Si. In contrast to p-Si−Os^{II}, it is present at all three monitoring wavelengths of 630, 700, and 800 nm. It is not present for p-Si−Os^{II} with 630-nm monitoring.

Emission decays of the derivatized sample were shorter than for p-Si and could be fit to the biexponential function in eq 4. From these fits τ_1 is nearly constant at ~30 ns at monitoring wavelengths throughout the emission manifold. τ_2 and the percent of PL contributed by τ_2 following 370-nm excitation

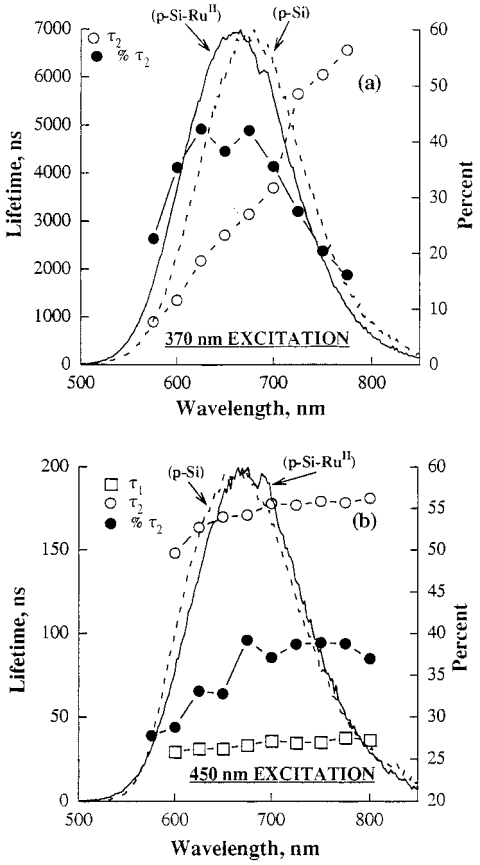

Figure 7. τ_2 (○) and percent of PL from τ_2 (●) by application of eq 4 to PL from p-Si derivatized with $[Ru(bpy)_2(4\text{-}CO_2H\text{-}4'Mebpy)](PF_6)_2$. Excitation at 370 nm (a) and 450 nm (b) with τ_1 is also shown (□). Similar results were obtained for τ_1 with excitation at 370 nm. Normalized emission spectra for p-Si (- - -) and the derivatized surface (—) are shown as references.

are shown plotted vs emission wavelength in Figure 7a. The percentage of emission by τ_2 increases on the blue side of the emission and roughly follows the emission profile of the underivatized surface. τ_2 increases from 1 to 7 μs as the monitoring wavelength is increased from 580 to 780 nm. Figure 7b is the analogue of Figure 7a showing the variations in τ_1 and τ_2 and percentage of light emitted by τ_2 at different monitoring wavelengths upon 450-nm excitation. The lifetimes are similiar to those for p-Si−Os^{II} with $\tau_1 \approx 32$ ns and $\tau_2 \approx 150-175$ ns. The percentage decay by τ_2 increases when the emission is monitored at low energy, but at any monitoring wavelength, decay times are an order of magnitude shorter than with excitation at 370 nm.

Other Derivatized Samples. Samples derivatized with *fac*-$[Re(bpy)(CO)_3(4\text{-}Etpy)](PF_6)$ and $[Zn(dmb)_3](PF_6)_2$ quenched the PL by ~70% and ~80%, respectively. Emission from these surfaces was *blue*-shifted by ~10 nm, and there was no evidence for an additional emission from the adsorbed complexes. Nanosecond components in the emission decays that were evident in the PL from the Os(II) and Ru(II) surfaces were absent in these samples. Only moderate decreases of 10−30% were observed in the average lifetimes relative to PL decays from bare, oxidatively etched p-Si.

No substantial quenching or lifetime changes were evident upon derivatization with either $4\text{-}CO_2H\text{-}4'$Mebpy or $9\text{-}AnCO_2H$. For the $9\text{-}AnCO_2H$/p-Si surface, UV excitation gave the characteristic green fluorescence of the anthracene, showing that the molecule was adsorbed.

Discussion

It is evident from our results that adsorption of polypyridyl complexes on anodized p-Si can lead to profound changes in photoluminescence properties. It is also clear that their adsorption causes a variety of effects depending on the absorbate. Adsorbed $9\text{-}AnCO_2H$ or $4\text{-}CO_2H\text{-}4'$Mebpy leave the PL relatively unaffected. The cations $[Zn(dmb)_3]^{2+}$ and $[Re(bpy)(CO)_3(4\text{-}Etpy)]^+$, which have no low-lying excited states, cause a slight (10 nm) blue shift and 20−30% decrease in lifetime but a significant decrease (60−80%) in emission intensity. For the adsorbed Ru^{II} and Os^{II} complexes, more profound effects are observed.

Surface Binding. The initial impetus for use of the carboxylic acid derivatized complexes was exploitation of surface binding either by ester formation (**1**) or H-bonding (**2**). However, a related, if less profound, effect was observed by using $[Os(bpy)_3](PF_6)_2$. There is no reason to believe that ester or H-bond formation to the surfaces does not play a role, but there must be other adsorption modes as well. Binding is not by simple precipitation. The surfaces were washed well with acetonitrile after exposure to solutions containing the adsorbates. Other surface-binding modes that may play a role include simple absorption with dispersion interactions with the surface and ion exchange by the cations, e.g., eq 5, although we have no spectrocopic evidence for the number of surface hydroxyl groups. Ion exchange would result in basic Si−O$^-$ sites at the surface interacting electrostatically with the cations.

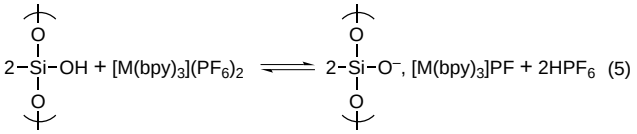

The extent of surface coverage is unknown, but on other oxide substrates (SiO_2, TiO_2, In_2O_3), coverage by $[Ru(bpy)_2(4\text{-}CO_2H\text{-}4'Mebpy)](PF_6)_2$ is known to be a monolayer or submonolayer.[21]

Photoluminescence Kinetic Model. As demonstrated by the data in Figures 1−3 and as shown in other work,[5,16,29−35] the PL properties of anodized p-Si are quite remarkable. The emission is excitation-wavelength-dependent with the emission profile moving to lower energy as the excitation energy is decreased from $\lambda = 310$ to 500 nm. The emission profile is time-dependent.

The PL of p-Si can be explained by a phenomenological model involving a distribution of emitters that are kinetically coupled by intersite energy transfer.[42] Important experimental observations that relate to this conclusion are the following: (1) the excitation energy dependence in Figure 1 suggests that there are discrete low-energy emitting sites selectively activated by low-energy excitation; (2) the low-energy sites have the longest lifetimes in the distribution of emitters (Figure 3); (3) the emission energy and emission profile are time-dependent, decreasing with time to resemble the spectra of the low-energy emitters.

These observations can be explained by invoking an energy-transfer cascade with energy transfer occurring from high- to low-energy emitters. Energy transfer would cause a decrease in apparent lifetime for the high-energy emitters because energy transfer is a decay pathway for these emitters. The lifetime of these emitters is the inverse of the sum of rate constants for "natural decay", k_0, and energy transfer, k_L, with $\tau = (k_0 + k_L)^{-1}$. A series of energy transfers by an energy-transfer cascade would explain the shift of the emission profile to lower energy

SCHEME 1

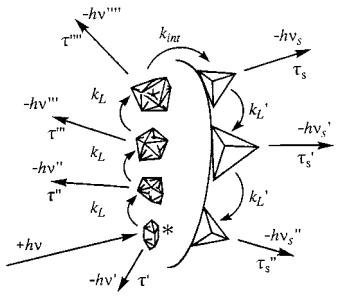

at longer lifetimes. With this interpretation, the decrease in PL energy with time provides a measure of the time scale for intersite energy transfer. Application of eq 2 to the data in Figure 2 gives $\tau_L \approx 22$ μs ($k_L \approx 4 \times 10^4$ s^{-1}).

Careful inspection of the excitation-dependent data in Figure 3 points to an additional complication. Excitation at 471 nm, at the red edge of the absorption, results in a marked decrease in the τ parameter of the distribution function in eq 3 and an equally marked decrease in the nonexponentiality parameter β. This points to the existence of a second set of even lower energy emitters. Given the marked decrease in β, the distribution of contributing emitters to this portion of the PL is very broad. These low-energy emitting sites must be kinetically uncoupled or weakly coupled to the energy-transfer cascade described above, which involves the higher-energy emitters. If energy transfer from the high-energy emitters were facile, the low-energy sites would dictate τ and, from the data in Figure 3, it would be ~10 μs rather than ~50 μs with 372-nm excitation.

There is further information in the experiments with adsorbed $[Zn(dmb)_3](PF_6)_2$ and $[Re(bpy)(CO)_3(4\text{-}Etpy)](PF_6)$, which have no low-lying excited states. For these adsorbates the integrated luminescence decreases by a factor of ~5, emission is slightly blue-shifted, and lifetimes are only slightly decreased. Similar results have been reported for surface quenching by a variety of bases and attributed to hole capture or to polarization effects.[12,14,15] These observations are consistent with the red, highly dispersed emission originating from surface or near-surface states whose excited-state properties are highly dependent on surface effects. The quenching mechanism by the adsorbed cations is not clear. On the basis of the ion-exchange model in eq 5, it could involve proton loss and self-quenching by Si−O$^-$ groups formed at the surface, for example.

The observations presented above lead to the phenomenological model in Scheme 1. Some of the important features of this model include the following.

(1) There is a distribution of interior emitters within the confines of the open, porous p-Si structures each with its own characteristic emission energy ($h\nu$) and decay lifetimes (τ). If the emission from the interior emitters originates from clusters or microparticles, the largest probably emit at the lowest energy.[9,43]

(2) Intersite energy transfer occurs by an energy-transfer cascade from highest- to lowest-energy emitters (k_L in Scheme 1). This is illustrated in Scheme 1 by energy tranfer from smaller to larger units. There is no significance to the polyhedral shapes chosen in the representation. The time scale for intersite energy transfer of ~22 μs is comparable to or shorter than the intrinsic time scale for excited-state decay from the emitting clusters or microparticles if they were isolated. They are not completely quenched because they contribute significantly to the PL.

(3) There are additional red emitters whose distribution is highly disperse. They are relatively low energy emitters ($h\nu_s$ in Scheme 1) with relatively short lifetimes and presumably undergo intersite energy transfer with rate constant k_L'. They appear to originate at or from the surface, since their excited-state properties are highly dependent on surface effects. They are only weakly coupled kinetically to the interior sites, and their formation by energy transfer from higher-energy internal emitters, k_{int} in Scheme 1, is slow on the time scale for decay ($k_{int}^{-1} < \tau''''$). In kinetic detail there are bound to be distributions of rate constants such as k_L and k_{int}. These labels provide a convenient summary of the average span of dynamical events that occur upon excitation.

The phenomenological model that we propose is consistent with the sample dependence of the PL from p-Si. PL energies and lifetimes would be predicted to be highly dependent on the distribution of cluster or microparticle sizes as would the energy-transfer rate constants that interconvert them. In this model the lowest-energy emitters are surface-localized, consistent with the known sensitivity of the PL to changes in the local environment.

Molecular Quenching by Adsorbed $[Os(bpy)_2(4\text{-}CO_2H\text{-}4'Mebpy)](PF_6)_2$. Surface adsorption of Os^{II} as $[Os(bpy)_2(4\text{-}CO_2H\text{-}4'Mebpy)](PF_6)_2$ or $[Os(bpy)_3](PF_6)_2$ leads to dramatic changes in the PL properties of anodized p-Si. As shown in the data in Figures 4 and 5, emission from p-Si is largely quenched and replaced by a red emission at $\lambda_{max} = 770$ nm, which originates from the MLCT excited state of the Os^{II} complex. This assignment follows from the excitation dependence in Figure 4 and the similarity in emission maximum with the complex in solution. There is some residual p-Si PL, but it is largely blue-shifted and greatly decreased in lifetime to ~165 ns compared with 10−50 μs for p-Si (Figure 3). That there are two separate contributors to the emission can be clearly discerned in the excitation spectra in Figure 4. Monitoring at or near the emission maximum reproduces the MLCT absorption spectrum in the visible with $\lambda_{max} \approx 470$ nm. For the residual emission to the blue, this feature is absent.

The PL decay data were fit to two components. These presumably represent averages of contributions of multiple emitters clustered around these emission time scales. The short-lived component with $\tau_1 \approx 23$ ns occurs on the time scale expected for excited-state decay from Os^{II}*. The other component at $\tau_2 \approx 165$ ns must originate from largely quenched, residual p-Si emission. This emission contributes significantly to the blue side of the emission as shown clearly by the wavelength dependence of τ_2 in Figure 5. Treating the data this way is highly qualitative. The biexponential fits to the data are reasonable, but there must be a distribution of emitters, and the decay constants are a reflection of the distributions, not of single species.

Since the complexes are presumably present in monolayer or submonolayer coverages, light absorption and excitation at 350 nm are dominated by p-Si. The appearance of Os^{II}* emission shows that the mechanism by which p-Si* is quenched is by energy transfer from p-Si* to the adsorbed complex. From the greatly decreased p-Si PL, energy transfer is rapid with $k_{en} \approx \tau_2^{-1} = 6 \times 10^6$ s^{-1} for the internal emitters. Once p-Si* → Os^{II} energy transfer occurs, Os^{II}* decay is rapid, $\tau_1 \approx 23$ ns, and its emission is shifted to the red.

The evidence for p-Si* → Os^{II} energy transfer is clear. Presumably, adsorption of Os^{II} causes quenching of the low-energy surface sites, as observed for $[Zn(dmb)_3](PF_6)_2$ and $[Re(bpy)(CO)_3(4\text{-}Etpy)](PF_6)$.

The quenching efficiency by Os^{II} is quite impressive. This is not surprising, since the time scale for p-Si* → Os^{II} energy

SCHEME 2

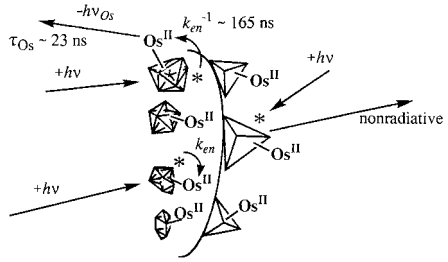

transfer, ~160 ns, is far shorter than the time scale for interparticle energy transfer, $\tau_L \approx 22\ \mu s$. This shows that the Os^{II} quenchers must penetrate into the relatively open, amorphous structures at the surface and be adsorbed onto *all* of the emitting internal sites. If this were not the case, there would be a residual p-Si PL with a lifetime of tens of microseconds. There is no way of knowing whether the red surface emitters contribute to the sensitization of Os^{II}* emission or are simply quenched.

A phenomenological kinetic quenching model consistent with these observations is illustrated in Scheme 2. As in Scheme 1, there is no significance to the polyhedral shapes used in the representation. In this model p-Si* → Os^{II} energy transfer is efficient but not especially rapid with $k_{en} \approx 6 \times 10^6\ s^{-1}$. Comparison with the unquenched lifetime data in Figure 3 reveals that the quenching efficiency $\eta \approx k_{en}/(k_{en} + \tau^{-1})$ is high, with $\eta \approx 1$.

The factors that dictate energy-transfer time scales at the molecular level have been explored for energy transfer from $[Os(bpy)_3]^{2+}$* and related Os^{II} MLCT excited states to the organic acceptors anthracene and tetracene.[44] They include the driving force ($-\Delta G°$), the quantum spacings and changes in equilibrium displacement for the coupled vibrations, and the energy-transfer matrix element. From the data in Figure 5 excitation of p-Si at 350 nm results in slightly enhanced p-Si* PL. This suggests that the quenching efficiency may fall for the highest-energy emitters. Further evidence comes from the data in Figure 4 where there is no evidence for Os^{II} in the excitation spectrum monitored at the highest emission energy (650 nm). In the earlier molecular-energy-transfer study mentioned above, a falloff in k_{en} was observed at high driving force and accounted for quantitatively by invoking the energy-transfer equivalent of the Marcus inverted region for electron transfer.[44] $\Delta G° \approx -0.4$ eV for energy transfer between the 0-μs PL for p-Si in Figure 2 and Os^{II}. The relevant energies are ~16 600 cm^{-1} (610 nm) for p-Si* and 13 000 cm^{-1} (770 nm) for Os^{II}*.

The properties of the molecular excited state once reached are relatively unaffected, although there is evidence for partial quenching. For $[Os(bpy)_3]^{2+}$ in acetonitrile at room temperature, $\tau = 60$ ns (deoxygenated) or 38 ns (aerated) and the emission quantum yield is $\Phi_{em} = 0.005$.[45] The Os^{II}* lifetime is ~23 ns on the surface.

Molecular Quenching by Adsorbed $[Ru(bpy)_2(4\text{-}CO_2H\text{-}4'Mebpy)](PF_6)_2$. There is evidence that related phenomena occur in p-Si to which $[Ru(bpy)_2(4\text{-}CO_2H\text{-}4'Mebpy)](PF_6)_2$ is adsorbed. The PL is excitation-dependent and, compared to that of p-Si, greatly quenched at all excitation wavelengths. Compared to p-Si, excitation of p-Si−Ru^{II} at 310 nm causes a slight red shift in PL, at 370 nm a slight blue-shift, and at 450 nm almost no shift (Figures 6 and 7). The emission that is observed is decreased in lifetime and depends in a complex way on excitation and monitoring wavelengths (Figure 7). In excitation spectra, Figure 6, there is clear evidence for MLCT absorption at ~450 nm showing that there is a Ru^{II}*-based MLCT contribution to the emission. This feature is observed with emission monitoring at 630, 700, and 800 nm.

The surface quenching mechanism for p-Si−Ru^{II} may be related to that for p-Si−Os^{II}, but there are significant differences in detail. For Os^{II}, adsorption of Ru^{II} probably results in the quenching of low-energy surface states. For adsorbed Ru^{II} there is a near energy match between the PL energy for the complex (680 nm, 1.47 eV) and the "average" p-Si-based PL at 650−710 nm (1.54−1.41 eV). In this case, there is the possibility that net energy transfer could occur in either direction: p-Si*−Ru^{II} → p-Si−Ru^{II}* or p-Si−Ru^{II}* → p-Si*−Ru^{II}.

Excitation at 450 nm and monitoring at 700 nm results in a short-lived decay that can be fit to the biexponential function in eq 4 with $\tau_1 \approx 32$ ns and $\tau_2 \approx 170$ ns. Excitation at 370 nm, where p-Si is nearly the sole absorber, and monitoring at 700 nm results in short- and long-lived components with $\tau_1 \approx 32$ ns and $\tau_2 \approx 4\ \mu s$. The latter is compared with typical lifetimes of 7−50 μs for underivatized p-Si (Figure 3).

Excitation at 450 nm results in only slight variations in τ_1 and τ_2 with monitoring wavelength (Figure 7b). It appears that the complex is the dominant emitter at this excitation wavelength. Emission from Ru^{II}* is longer-lived than from Os^{II}* with $\tau \approx 100-150$ ns on the surface, but it still appears to be partly quenched. $\tau = 0.9\ \mu s$ for the complex in deaerated acetonitrile. The measured PL lifetime is comparable to the average lifetime of ~100 ns for the same excited state on SiO_2.[22]

There appear to be p-Si*−Ru^{II} sites at lower energy compared with Ru^{II}*. From the lifetime data in Figure 7a, τ_2 increases with monitoring wavelength. It continues to increase past the emission maximum for Ru^{II}* and reaches 6−7 μs at 790 nm. For underivatized p-Si, $\tau \approx 50\ \mu s$ at this wavelength (Figure 3).

At the emission maximum for Ru^{II}* (Figure 7a), $\tau_2 \approx 3\ \mu s$ with 370-nm (p-Si) excitation. This is a decrease in τ for p-Si* emission from underivatized p-Si by a factor of ~10. The quenching mechanism is presumably the same: p-Si*−Ru^{II} → p-Si−Ru^{II}* energy transfer followed by relatively rapid Ru^{II}* decay. With this interpretation energy transfer to Ru^{II} is efficient with $\eta \approx k_{en}/(k_{en} + \tau^{-1}) \approx 0.9$ and $\tau_{en} \approx 3\ \mu s$. The decrease in k_{en} for adsorbed Ru^{II} ($k_{en} \approx 3 \times 10^5\ s^{-1}$) compared with that of adsorbed Os^{II} ($k_{en} \approx 6 \times 10^6\ s^{-1}$) is consistent with the change in driving force from $\Delta G° \approx -0.4$ eV for Os^{II} to $\Delta G° \approx 0$ for Ru^{II}. With this interpretation, excitation of high-energy interior sites is followed by p-Si*−Ru^{II} → p-Si−Ru^{II}* energy transfer. Excitation of Ru^{II} adsorbed onto low-energy sites is followed by p-Si−Ru^{II}* → p-Si*−Ru^{II} energy transfer.

Conclusion

Our results point to a range of dynamic photophysical processes in anodized p-Si. There is phenomenological evidence for internal intercluster energy transfer and kinetically weak, uncoupled surface emitting sites at lower energy. Surface adsorption, by ester formation, H-bonding, or ion exchange, leads to quenching of emission from the surface states. Surface adsorption of polypyridyl complexes of Ru^{II} and Os^{II} leads to dynamic energy interchange between p-Si and the adsorbed complex by p-Si*-M^{II} → p-Si-M^{II}* energy transfer. Since the MLCT excited states are relatively short-lived, this leads to an efficient quenching mechanism for PL from p-Si. For adsorbed Os^{II} the MLCT state is lower-lying by ~0.4 eV, $\tau_{en} \approx 160$ ns ($k_{en} \approx 6 \times 10^6\ s^{-1}$), and energy transfer is nearly complete except for the highest-energy p-Si emitters. For Ru^{II}, $\Delta G° \approx 0$ eV. Energy transfer is slower, $\tau_{en} \approx 3\ \mu s$ ($k_{en} \approx 3 \times 10^5\ s^{-1}$), and can occur in either direction p-Si*−Ru^{II} ↔ p-Si−

Ru^{II}* depending on the excited-state energy of the internal site. Net quenching is still ~90% complete.

The efficiency of energy transfer and greatly decreased lifetimes for derivatized p-Si are consistent with an open, porous microstructure with the adsorbed complex distributed throughout. The complexes are presumably adsorbed onto p-Si microparticles or clusters having a range of sizes. The high-energy transfer efficiencies and high absorptivity of p-Si as a substrate raise the interesting possibility of using its microporous surface structure as an "antenna" array for the sensitization of energy conversion processes in adsorbed molecular assemblies.

Acknowledgment. This work was supported by the U.S. Army Research Office through Grant DAAH04-95-1-0144.

References and Notes

(1) Canham, L. T. *Appl. Phys. Lett.* **1990**, *57*, 1046.
(2) Bsiesy, A.; Vial, J.; Gasparad, F.; Herino, R.; Ligeon, M.; Muller, F.; Romestain, R.; Wasiela, A.; Maimaoui, A.; Bomchil, G. *Surf. Sci.* **1991**, *254*, 195.
(3) Lehmann, V.; Gosele, U. *Appl. Phys. Lett.* **1991**, *58*, 856.
(4) Sailor, M. J.; Kavanagh, K. L. *Adv. Mater.* **1992**, *4*, 432.
(5) Brandt, M.; Fuchs, H.; Stutzmann, M.; Weber, J.; Cardona, M. *Solid State Commun.* **1992**, *81*, 307.
(6) Prokes, S.; Carlos, W.; Bermudez, V. *Appl. Phys. Lett.* **1992**, *61*, 1447.
(7) Delerue, C.; Lannoo, M.; Allan, G. *J. Lumin.* **1993**, *57*, 249.
(8) Takeda, Y.; Hyodo, S.; Suzuki, N.; Motochiro, T.; Hioki, T.; Noda, S. *J. Appl. Phys.* **1993**, *73*, 1924.
(9) Brus, L. *J. Phys. Chem.* **1994**, *98*, 3575.
(10) Prokes, S. M. *Electrochem. Soc. Interface* **1994**, 41.
(11) Koch, F.; Petrova-Koch, V.; Muschik, T. *J. Lumin.* **1993**, *57*, 271.
(12) Lauerhaas, J. M.; Credo, G. M.; Heinrich, J. L.; Sailor, M. J. *J. Am. Chem. Soc.* **1992**, *114*, 1911.
(13) Fisher, D. L.; Harper, J.; Sailor, M. J. *J. Am. Chem. Soc.* **1995**, *117*, 7846.
(14) Chun, J. K. M.; Bocarsly, A. B.; Cottrell, T. R.; Benziger, J. B.; Yee, J. C. *J. Am. Chem. Soc.* **1993**, *115*, 3024.
(15) Canham, L. T. *Appl. Phys. Lett.* **1993**, *63*, 337.
(16) Ko, M. C.; Meyer, G. *Chem. Mater.* **1995**, *7*, 12.
(17) Sweryda-Krawiec, B.; Coffer, J. L. *J. Electrochem. Soc.* **1995**, *142*, L93.
(18) Andsager, D.; Hilliard, J.; Hetrick, J. M.; AbuHassan, L. H.; Plisch, M.; Nayfeh, M. H. *J. Appl. Phys.* **1993**, *74*, 4783.
(19) Andsager, D.; Hilliard, J.; Nayfeh, M. H. *Appl. Phys. Lett.* **1994**, *64*, 1141.
(20) Coffer, J. L. *J. Lumin.* **1996**, *70*, 343.
(21) Gerfin, T.; Grätzel, M.; Walder, L. In *Progress in Inorganic Chemistry*; Karlin, K., Ed.; John Wiley: New York, 1997; Vol. 44, p 345.
(22) (a) Meyer, T. J.; Meyer, G. J.; Pfennig, B. W.; Schoonover, J. R.; Timpson, C. J.; Wall, J. F.; Kobush, C.; Chen, X.; Peek, B. M.; Wall, C. G.; Ou, W.; Erickson, B. W.; Bignozzi, C. A. *Inorg. Chem.* **1994**, *33*, 3952. (b) Pfenning, B. W.; Chen, P.; Meyer, T. J. *Inorg. Chem.* **1996**, *35*, 2898.
(23) Jung, K. H.; Shih, S.; Kwong, D. L. *J. Electrochem. Soc.* **1993**, *140*, 3046.
(24) Peek, B. M.; Ross, G. T.; Edwards, S. M.; Meyer, G. J.; Meyer, T. J.; Erickson, B. W. *Int. J. Pept. Protein Res.* **1991**, *38*, 114.
(25) Buckingham, D. A.; Dwyer, F. P.; Goodwin, H. A.; Sargeson, A. M. *Aust. J. Chem.* **1964**, *17*, 325.
(26) Caspar, J. V.; Meyer, T. J. *J. Phys. Chem.* **1983**, *87*, 952.
(27) Meyer, T. J.; Sullivan, B. P.; Caspar, J. V. *Inorg. Chem.* **1987**, *26*, 4145.
(28) Mott, N. F.; Davis, E. A. *Electronic Processes in Noncrystalline Materials*, 2nd ed.; Oxford University Press: Oxford, 1979.
(29) Pavesi, L.; Ceschini, M.; Rossi, F. *J. Lumin.* **1993**, *57*, 131.
(30) Stutzmann, M.; Weber, J.; Brandt, M. S.; Fuchs, H. D.; Rosenbauer, M.; Deak, P.; Hopner, A.; Breitschwerdt, A. *Adv. Solid State Phys.* **1992**, *32*, 179.
(31) Laiho, R.; Pavlov, A.; Tsuboi, T. *J. Lumin.* **1993**, *57*, 89.
(32) Finkbeiner, S.; Weber, J.; Rosenbauer, M.; Stutzmann, M. *J. Lumin.* **1993**, *57*, 231.
(33) Ookubo, N.; Ono, H.; Ochiai, Y.; Mochizuki, Y.; Matsui, S. *Appl. Phys. Lett.* **1992**, *61*, 940.
(34) Chen, X.; Henderson, B.; O'Donnel, K. P. *Appl. Phys. Lett.* **1992**, *60*, 2672.
(35) Klafter, J.; Shlesinger, M. F. *Proc. Natl. Acad. Sci. U.S.A.* **1986**, *83*, 848.
(36) Kohlrausch, R. *Annalen* **1847**, *5*, 430.
(37) Williams, G.; Watts, D. C. *Trans. Faraday Soc.* **1971**, *66*, 80.
(38) Palmer, R. K.; Stein, D.; Abrahams, E. S.; Anderson, P. W. *Phys. Rev. Lett.* **1984**, *53*, 958.
(39) Scher, H.; Shlesinger, M. F.; Bendler, J. T. *Phys. Today* **1991**, *588*, 26 and references therein.
(40) Calcott, P. D. J.; Nash, K. J.; Canham, L. T.; Kane, M. J.; Brumhead, D. *J. Phys.: Condens. Matter* **1993**, *5*, L91.
(41) Calcott, P. D. J.; Nash, K. J.; Canham, L. T.; Kane, M. J.; Brumhead, D. *Mater. Res. Symp. Proc.* **1993**, *283*, 143.
(42) Fisher, D. L.; Gamboa, A.; Harper, J.; Lauerhaas, J. M.; Sailor, M. J. *Mater. Res. Soc. Symp. Proc.* **1995**, *358*, 507.
(43) Littau, K. A.; Szajowski, P. J.; Muller, A. J.; Kortan, A. R.; Brus, L. E. *J. Phys. Chem.* **1993**, *97*, 1224.
(44) Murtoza, Z.; Graff, D. K.; Pipp, A. P.; Worl, L. A.; Jones, J. W. E.; Bates, W. D.; Meyer, T. J. *J. Phys. Chem.* **1994**, *98*, 10504.
(45) Kober, E. M.; Caspar, J. V.; Lumpkin, R. S.; Meyer, T. J. *J. Phys. Chem.* **1986**, *90*, 3722.